The Plant Cell, Vol. 17, 3066–3080, November 2005, www.plantcell.org

Selective Membrane Protein Internalization Accompanies Movement from the Endoplasmic Reticulum to the Protein Storage Vacuole Pathway in *Arabidopsis*

Mohammed Oufattole,[a] Joon Ho Park,[a] Marianne Poxleitner,[a] Liwen Jiang,[b] and John C. Rogers[a,1,2]

[a] Institute of Biological Chemistry, Washington State University, Pullman, Washington 99163
[b] Department of Biology, Chinese University of Hong Kong, Shatin, New Territories, Hong Kong, China

In plant cells, certain membrane proteins move by unknown mechanisms directly from the endoplasmic reticulum (ER) to prevacuolar or vacuole-like organelles where membrane is internalized to form a dense, lattice-like structure. Here, we identify a sequence motif, PIEPPPHH, in the cytoplasmic tail of a membrane protein that directs the protein from the ER to vacuoles where it is internalized. A type II membrane protein in *Arabidopsis thaliana*, (At)SRC2 (for Soybean Gene Regulated by Cold-2), binds specifically to PIEPPPHH and moves from the ER to the same vacuoles where it is internalized. Not all proteins that move in this pathway are internalized because another *Arabidopsis* type II membrane protein, (At)VAP (for Vesicle-Associated Protein), localizes to the same organelles but remains exposed on the limiting membrane. The identification of (At)SRC2 and its preference for interaction with a targeting motif specific for the ER-to-vacuole pathway may provide tools for future dissection of mechanisms involved in this unique trafficking system.

INTRODUCTION

Movement of membrane proteins within the secretory pathway of plant cells is complex because plant cells may contain different types of vacuoles (Hoh et al., 1995; Paris et al., 1996; Di Sansebastiano et al., 1998, 2001; Park et al., 2004), and proteins may move to vacuoles via the Golgi apparatus (Jiang and Rogers, 1998; Hinz et al., 1999; Hillmer et al., 2001) or directly from the endoplasmic reticulum (ER; Hara-Nishimura et al., 1998; Jiang and Rogers, 1998; Jiang et al., 2000). Traffic in pathways to the protein storage vacuole (PSV) is particularly complex (Vitale and Hinz, 2005). In developing legume embryo cells (Hinz et al., 1999; Hillmer et al., 2001) as well as in developing wheat (*Triticum aestivum*) endosperm early during development (Kim et al., 1988), storage proteins form aggregates within the Golgi that bud off as dense vesicles for transport to the PSV (reviewed in Vitale and Hinz, 2005). In other systems, a direct ER-to-PSV pathway has been described, where intermediate organelles, termed precursor-accumulating (PAC) vesicles, apparently form by budding directly from the ER but then receive vesicular traffic from the Golgi (Hara-Nishimura et al., 1998).

PAC vesicles were defined at the ultrastructural level by observing electron-dense aggregates of protein within the ER lumen that then appeared to be transferred to large vesicles free within the cytoplasm. The ER aggregates and electron-dense centers of PAC vesicles both contained storage proteins that were subsequently deposited within PSVs (Hara-Nishimura et al., 1998). Because storage protein traffic and PSVs are particularly prominent in developing seeds, study of PAC vesicles has largely been performed in those tissues, particularly in developing pumpkin (*Cucurbita* sp) and castor bean (*Ricinus communis*) seeds (Hara-Nishimura et al., 1998; Mitsuhashi et al., 2001). However, other strategies that induce abnormal deposits of proteins within the ER result in their transfer to PAC vesicle-like structures in the cytoplasm (Hayashi et al., 1999; Kinney et al., 2001), and some hydrolytic enzymes are transferred via large vesicles that bud directly from ER to vacuoles that are activated to digest storage proteins in germinating seeds (reviewed in Herman and Schmidt, 2004).

Little is known of the mechanisms by which PAC vesicles form from the ER, but precedents from studies of budding of transport vesicles indicate that specific integral membrane proteins within the ER membrane would probably be recognized by cytoplasmic coat proteins to drive vesicle formation, while lumenal domains of the membrane proteins would bind cargo molecules for transfer into the vesicles (Robinson et al., 1998). We identified a chimeric reporter protein, termed Re-F-B-α, that moved from ER to PSVs without transiting the Golgi (Jiang and Rogers, 1998). The criteria for determining absence of Golgi traffic were that Re-F-B-α in the vacuole fraction did not acquire complex glycans, whereas a reporter with the same lumenal and transmembrane domains but with a different cytoplasmic tail, termed Re-F-B-B, that trafficked to a lytic compartment did acquire complex glycans (Jiang and Rogers, 1998). Additionally, when provided with the necessary lumenal cleavage sites, Re-F-B-B was cut by a Golgi-localized Kex2 protease, whereas Re-F-B-α was not (Jiang

[1] Current address: National Science Foundation, 4201 Wilson Boulevard, Arlington, VA 22230.
[2] To whom correspondence should be addressed. E-mail jrogers@nsf.gov; fax 703-292-9061.
The author responsible for distribution of materials integral to the findings presented in this article in accordance with the policy described in the Instructions for Authors (www.plantcell.org) is: John C. Rogers (jrogers@nsf.gov).
Article, publication date, and citation information can be found at www.plantcell.org/cgi/doi/10.1105/tpc.105.035212.

and Rogers, 1999). In transgenic tobacco (*Nicotiana tabacum*) plants, Re-F-B-α entered ~0.5-μm-diameter cytoplasmic vesicles, where it, together with two integral membrane proteins, a tonoplast intrinsic protein isoform termed Dark-Induced Protein (DIP) and a receptor-like protein termed RMR protein, reached the organelles by traffic through the Golgi. These organelles, and similar organelles in wild-type plants that lacked Re-F-B-α but contained DIP and RMR proteins, delivered their contents to developing PSVs in seeds (Jiang et al., 2000). They morphologically were indistinguishable from PAC vesicles (Hara-Nishimura et al., 1998), and their electron-dense internal contents carrying the integral membrane proteins were released into the lumens of developing PSVs where they aggregated with other electron-dense material to form an internal structure termed the PSV crystalloid (Jiang et al., 2000). Immunofluorescence and immunoelectron microscopy confirmed that PSV crystalloid contained the three integral membrane proteins, DIP was preferentially localized to crystalloid biochemically purified from pumpkin (Jiang et al., 2000) and tomato (*Lycopersicon esculentum*) PSVs (Jiang et al., 2001), and the crystalloid fraction was enriched in lipid (Jiang et al., 2000). Thus, the crystalloid represents some unusual sort of arrangement of membranes; its lattice-like structure from freeze fracture studies (Lott, 1980) indicates that it may be organized from parallel membrane arrays.

The type I Re-F-B-α reporter protein appeared to offer a probe for the pathway because its relatively simple 17–amino acid cytoplasmic tail directed its traffic (Jiang and Rogers, 1998). Here, we demonstrate that the sequence PIEPPPHH within the cytoplasmic tail sequence is necessary and sufficient to direct the protein into the ER-to-PSV pathway, and mutations within the sequence resulted in movement of the protein through the Golgi to a lytic compartment. The Re-F-B-α cytoplasmic tail represents the C-terminal cytoplasmic tail of the tonoplast intrinsic protein α-TIP, one of the markers for the limiting membrane of the PSV (Jauh et al., 1999). Full-length α-TIP expressed in suspension culture protoplasts also moves to PSV-like structures where it can be on the limiting membrane as well as internalized. Deletion of PIEPPPHH from the α-TIP cytoplasmic tail causes it to move to vacuoles with characteristics of lytic vacuoles as well as to the tonoplast of the central vacuole. Thus, PIEPPPHH appears to function as an ER-to-PSV targeting signal within its native context.

Here, we identify an *Arabidopsis thaliana* type II ER membrane protein, termed (At)SRC2 (for Soybean Gene Regulated by Cold-2), that binds to the sequence PIEPPPHH preferentially over the sequence HQPLATEDY and moves together with Re-F-B-α from ER to vacuoles. Movement is accompanied by membrane internalization such that (At)SRC2 is protease sensitive when localized to the ER membrane but fully protected from exogenous protease when present in a vacuole fraction. Consistent with these results from transient expression experiments that indicate its incorporation into internalized membrane, (At)SRC2 is present in crystalloid-like structures within PSVs in mature *Arabidopsis* seeds. These results tie (At)SRC2 closely to the process by which membrane moves from ER to vacuoles, accompanied by its internalization, and raise the question of a possible role for (At)SRC2 in the budding of PAC vesicles from the ER.

RESULTS

Definition of the Sequence in Re-F-B-α Responsible for ER-to-PSV Targeting

When the C-terminal cytoplasmic tail sequences from different tonoplast intrinsic protein isoforms were compared, α-TIP proteins were observed to contain an additional, conserved sequence adjacent to the last transmembrane domain (Figure 1, underlined). We therefore tested the role of this α-TIP–specific sequence in targeting Re-F-B-α into the ER-to-PSV pathway. We made a series of constructs containing Re-F-B fused, at its C terminus, to one of the following sequences derived from *Phaseolus vulgaris* α-TIP: PIEPPPHH, HQPLAPEDY, and three mutated variants of PIEPPPHH (AAAPPPHH, PIEPPPAA, and PIEAAAHH). Re-F-B-B and Re-F-B-α, containing full BP-80 and α-TIP cytoplasmic tail sequences, respectively, were used as controls. These seven constructs were separately expressed in tobacco protoplasts. Cells were labeled with [^{35}S]Met + Cys and separated into soluble and membrane fractions, and the products derived from the reporter proteins were immunoprecipitated with antialeurain antibodies (Figure 2).

As shown previously (Jiang and Rogers, 1998), full-length Re-F-B-B was predominantly selected in the membrane fraction as indicated by the doublet of ~47 and 50 kD (Figure 2, lane 1M; position indicated by arrow to right). The soluble fraction contains a small amount of full-length doublet because of contamination with membrane that does not pellet at 13,000*g* (Jiang and Rogers, 1998). The soluble fraction also shows two additional proteins at ~35 and 32 kD (Figure 2, lane 1S; indicated by dot) that correspond to aleurain resulting from proteolytic processing of the reporter in the lytic prevacuolar compartment/vacuole (Jiang and Rogers, 1998). The appearance of these bands is specific biochemical evidence that the reporter protein reached a lytic compartment. When the BP-80 cytoplasmic tail sequence was replaced by the full-length α-TIP sequence, PIEPPPHHHQPLAPEDY, only full-length Re-F-B-α was selected (lanes 2S and

TIP	Species	Access#	*TMD*	Cytoplasmic CT
DIP :	Ar	AF367283	..*GLIYGDVFI*	--------GSYAPAPTTESYP
	Sn	X70417	..*GFIYGDVFI*	--------TAGAOKOTSEDTA
Delta:	Ar	U39485	..*GLIQGNVFM*	--------GSSEHVPLASADF
	Co	U62778	..*GLIYGNVFM*	----------NSDHAPLSNDF
	Su	X95950	..*GLIYPNVFI*	----------SNEHIPLTNEY
Gamma:	Ar	M84344	..*GLIYEVFFI*	---------NTTHEQLPTTDY
	Ra	D84669	..*GLIYEFVFI*	--------NQNGHEQLPTTDY
	Ba	X80266	..*GVIYELLFI*	---------SRTHEQLPTTDY
Alpha:	Ar	M84343	..*ALIYEYMVI*	PTEPPTHHAHGVHQPLAPEDY
	Ph	X62873	..*ALVYEYAVI*	PIEPPPHH----HQPLAPEDY

Figure 1. Comparison of C-Terminal Sequences of Different TIP Isoforms.

A portion of the transmembrane domain (italics) and the cytoplasmic C terminus (CT) are shown for each. A conserved motif specific to α-TIP family members is underlined. Species and accession numbers are indicated for each sequence: Ar, *Arabidopsis*; Sn, snapdragon (*Antirrhinum majus*); Co, cotton (*Gossypium hirsutum*); Su, sunflower (*Helianthus annuus*); Ra, radish (*Raphanus sativus*); Ba, barley (*Hordeum vulgare*); Ph, *Phaseolus vulgaris*.

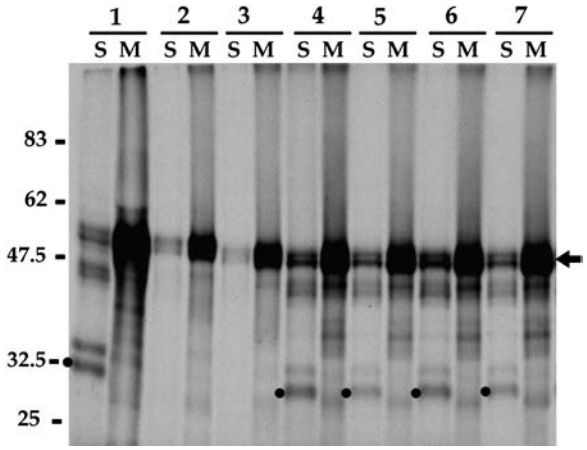

Figure 2. Effects of Modified α-TIP C-Terminal Sequences on Targeting Specificity of the Reporter Protein.

Protoplasts were transformed with several variants of the reporter gene differing in the sequences of their cytoplasmic tails: (1) wild-type BP-80 C terminus, (2) PIEPPPHHHQPLAPEDY, (3) PIEPPPHH, (4) HQPLATEDY, (5) AAAPPPHH, (6) PIEPPPAA, and (7) PIEAAAHH. Cells were continuously labeled with [^{35}S]Met + Cys for 2 h, separated into soluble (S) and membrane (M) fractions, and immunoprecipitated using antialeurain antibodies. The immunoprecipitated proteins were separated by SDS-PAGE and detected by fluorography. Arrow, full-length reporter protein; dots, soluble processed mature barley aleurain. Positions of molecular mass standards are indicated in kilodaltons at left.

2M), and no mature aleurain was present in the soluble fraction. Thus, Re-F-B-α did not reach a lytic compartment. Instead, as shown previously, it exits the ER and moves to 0.5- to 1-μm cytoplasmic vacuoles that are separate from organelles on the lytic vacuole pathway (Jiang and Rogers, 1998). When the α-TIP–specific sequence, PIEPPPHH, was fused at the C terminus of Re-F-B (lanes 3S and 3M), it resulted in a profile similar to that of Re-F-B-α; no processing of the proaleurain moiety occurred. This processing profile reappeared in the soluble fraction, however, when HQPLAPEDY (lane 4S) or any of the mutated forms of PIEPPPHH (AAAPPPHH [lane 5S], PIEPPPAA [lane 6S], or PIEAAAHH [lane 7S]) was used. These results show that only PIEPPPHH was able to functionally replace the full-length α-TIP cytoplasmic tail and prevent the reporter protein from reaching the lytic vacuole. We therefore hypothesized that PIEPPPHH contains a positive signal that is recognized by cytoplasmic proteins whose interaction diverts the reporter away from an ER-to-Golgi to a lytic vacuole pathway.

PIEPPPHH Controls Movement of Intact α-TIP

To test the possibility that the role of PIEPPPHH was an artifact generated using a chimeric reporter protein, we prepared constructs consisting of full-length α-TIP, or α-TIP with PIEPPPHH deleted from its C-terminal cytoplasmic tail, as fusions with enhanced green fluorescent protein (GFP) at their cytoplasmic N termini. These two fusion proteins, termed GFPαTIP and GFPαTIPΔ, respectively, were expressed in protoplasts; the cell vacuolar fraction was separated from the pellet containing the rest of the cell membranes, including ER and Golgi, and the distribution of α-TIP was detected on an immunoblot (Figure 3). For GFPαTIP, only a trace of full-length fusion protein was present in the pellet fraction (arrow); the remainder of the protein had been cleaved to yield an ~26-kD band that was distributed similarly between pellet and vacuolar fractions. It previously has been shown that α-TIP may be proteolytically cleaved within the first lumenal loop to yield a product of similar size (Inoue et al., 1995); the intracellular site(s) at which this cleavage occurs is not known. By contrast, the amount of full-length GFPαTIPΔ protein in the pellet fraction was similar to the amount of the ~26-kD product, and an appreciable amount of precursor was also detected in the vacuolar fraction (Figure 3, lanes 5 and 6, arrows). In addition, a second ~23-kD proteolytic product (asterisk) was present in the vacuolar fraction in amounts similar to that for the ~26-kD band. The relative abundance of this ~23-kD band indicates that a substantial portion of GFPαTIPΔ traffics to a vacuolar destination that has proteolytic activity different from that in the destination of full-length GFPαTIP.

The intracellular distributions of the two fusion proteins were studied by microscopy. We found that protoplasts expressing either of the proteins were unusually fragile such that they were easily broken during transport in Petri dishes to the confocal microscopy facility. In addition, when visualized in the laboratory using wide-field fluorescence microscopy (Jauh et al., 1998), GFP-expressing cells were abundant 16 h after electroporation, but by 20 h the number of cells had decreased substantially. Their fragility appeared to correlate with unusually large size as compared with protoplasts transformed with other non-TIP proteins (data not shown), and we interpret their phenotypes to

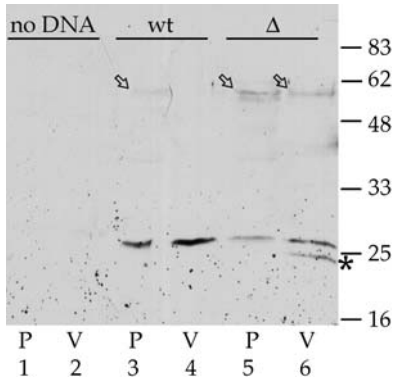

Figure 3. Subcellular Fractionation of GFP-αTIP Fusion Proteins Expressed in Protoplasts.

Protoplasts were transfected with no DNA (lanes 1 and 2), with GFPαTIP expression plasmid DNA (wt, lanes 3 and 4), or with GFPαTIPΔ expression plasmid DNA (Δ, lanes 5 and 6). Seventeen hours later, protoplasts were harvested and separated into pellet (P) and vacuole (V) fractions. Aliquots representing 10% of each fraction were separated on a 4 to 20% acrylamide gradient SDS-PAGE gel, transferred to nitrocellulose, and α-TIP protein detected with a 1:2000 dilution of anti-α-TIP protein antiserum. Arrows, full-length fusion protein; asterisk, ~23-kD proteolytic product specific for GFPαTIPΔ. Positions of molecular mass markers are indicated in kilodaltons at right.

indicate an adverse effect caused by aquaporin activity of the expressed α-TIP proteins. Both proteins were present in patterns consistent with that of ER. For GFPαTIP expressed alone, 37/38 cells imaged additionally showed GFP fluorescence in vacuole-like structures separate from ER. A common pattern is shown in Figure 4A, where the protein was associated with convoluted structures that frequently appeared filled with fluorescent protein (arrow) as well as vacuoles above the nucleus that have open lumens but with walls of varying thickness. For the structure indicated by the arrow, multiple optical sections taken at 0.5-μm steps failed to define a lumen (data not shown), indicating that GFP had been internalized into a vacuole-like organelle. Another common pattern in Figure 4B shows the protein in a broad perinuclear network that appears bubbly, indicating the presence of many small vacuoles. For GFPαTIPΔ expressed alone, 33/43 cells imaged showed the protein in vacuole-like structures as well as in a typical ER-like pattern. These vacuole-like structures ranged from discrete, well-defined vacuoles (Figure 4C, arrow) to a broad network in the perinuclear area (Figure 4D) to numerous bright punctate structures distributed throughout the cell (Figure 4E).

To define further the distribution of the two proteins within vacuolar organelles, we compared their localization to that for a reporter protein comprised of proaleurain fused to the transmembrane domain and cytoplasmic tail from an *Arabidopsis* isoform of BP80 [termed VSR_{At1} (Paris et al., 1997) or (At)BP80b (Hadlington and Denecke, 2000)], where monomeric red fluorescent protein (mRFP; Campbell et al., 2002) was inserted into the cytoplasmic tail. This protein, termed (At)BP80b-mRFP, trafficked normally to a lytic compartment destination as judged from the fact that its proaleurain moiety was proteolytically processed to yield mature aleurain indistinguishable in size from that derived from Re-F-B-B (data not shown). Sixteen cells coexpressing GFPαTIP plus (At)BP80b-mRFP and 15 cells coexpressing GFPαTIPΔ plus (At)BP80b-mRFP were studied. Coexpression of the second protein did not alter the localization pattern for the GFP fusion proteins. For all GFPαTIP cells, (At)BP80b-mRFP was present predominantly in ER and in bright punctate organelles (e.g., Figure 4B) that were mobile; their appearance is consistent with that for both Golgi and prevacuolar compartments (Li et al., 2002). No association of GFPαTIP and (At)BP80b-mRFP was observed. For nine GFPαTIPΔ cells, (At)BP80b-mRFP gave a similar pattern (e.g., Figure 4D), while in six cells, the two proteins were colocalized on numerous round and elongated structures ranging in size up to 1 μm diameter (e.g., Figure 4E, where colocalization is indicated by yellow color). Additionally, for both sets of experiments, the presence of a red background in ER allowed better visualization of the central vacuole tonoplast. In none of the GFPαTIP cells was GFP associated with that tonoplast, while in four of the GFPαTIPΔ cells, clear labeling of the tonoplast was present (Figures 4D and 4E, arrows). These results together demonstrate that GFPαTIPΔ traffics to a vacuolar destination differently from GFPαTIP: (1) it is proteolytically processed to a differently sized product, (2) it is frequently present together with (At)BP80b-mRFP in organelles similar in appearance to prevacuolar compartments, and (3) it frequently is visualized on central vacuole tonoplast. These results are fully consistent with those presented for the Re-F-B-α reporter protein and indicate that PIEPPPHH is important for proper trafficking of full-length α-TIP.

Screening for Potential PIEPPPHH Interacting Proteins

To identify proteins that interact specifically with PIEPPPHH, we performed a yeast two-hybrid screen (Luban and Goff, 1995) where three tandemly repeated units of the sequence were used as bait to screen an *Arabidopsis* cDNA library. Positive clones were selected based on their ability to grow on medium lacking His and adenine as well as their expression of α- or β-galactosidase. Among 150 positive clones initially identified, 28, representing seven different cDNAs, interacted with the PIEPPPHH × 3 bait protein but not with a control bait protein carrying PIEAAAHH × 3 or a bait protein carrying a human lamin C sequence (data not shown); these were studied further. Three are proteins with unknown functions: At3g13060 (seven isolates), At1g26920 (three isolates), and At1g68310 (one isolate). One, At1g72150, has a Sec14/CRAL-TRIO domain associated with phosphatidylinositol binding (Sha et al., 1998). One, X67816, encodes a cinnamyl alcohol dehydrogenase. Two are the focus of this article: At1g09070 (14 isolates) represents an *Arabidopsis* equivalent of soybean (*Glycine max*) SRC2 (Takahashi and Shimosaka, 1997), and At3g60600 (one isolate) is a VAP33 homolog (Skehel et al., 1995; Laurent et al., 2000) that serves as a parallel control for the (At)SRC2 studies presented here. These two *Arabidopsis* proteins are designated (At)SRC2 and (At)VAP, respectively.

Both (At)SRC2 and (At)VAP were predicted to be type II integral membrane proteins, each comprised of a long cytoplasmic N-terminal region, a transmembrane domain, and a short lumenal domain. The N terminus of (At)SRC2 is comprised of a C2 domain, a calcium-regulated phospholipid binding domain (Rizo and Südhof, 1998), and the protein's central cytoplasmic domain contains seven repeats rich in Pro, Gly, Tyr, and Gln. The cytoplasmic domain of (At)VAP has a predicted coiled coil region adjacent to the transmembrane domain that, in an animal system, was shown to be involved in interactions with a v-SNARE (Skehel et al., 1995) and a well conserved N-terminal domain homologous to the major sperm protein from nematodes, a domain believed to participate in the formation of a protein–protein network (Laurent et al., 2000).

To characterize (At)SRC2 and (At)VAP further, we raised polyclonal antibodies against recombinant proteins representing portions of their cytoplasmic domains and also to synthetic peptides whose sequences matched other regions of the cytoplasmic domains. The specificity of the antibodies is documented in subsequent figures.

In Vitro Binding Assays

The yeast two-hybrid results indicated that both (At)SRC2 and (At)VAP interacted specifically with the sequence PIEPPPHH. The specificity of this interaction was further tested using recombinant proteins expressed in tobacco protoplasts. Truncated forms of the two proteins representing their cytoplasmic domains carrying six C-terminal His residues were expressed in tobacco protoplasts, purified from cell extracts by chromatography on

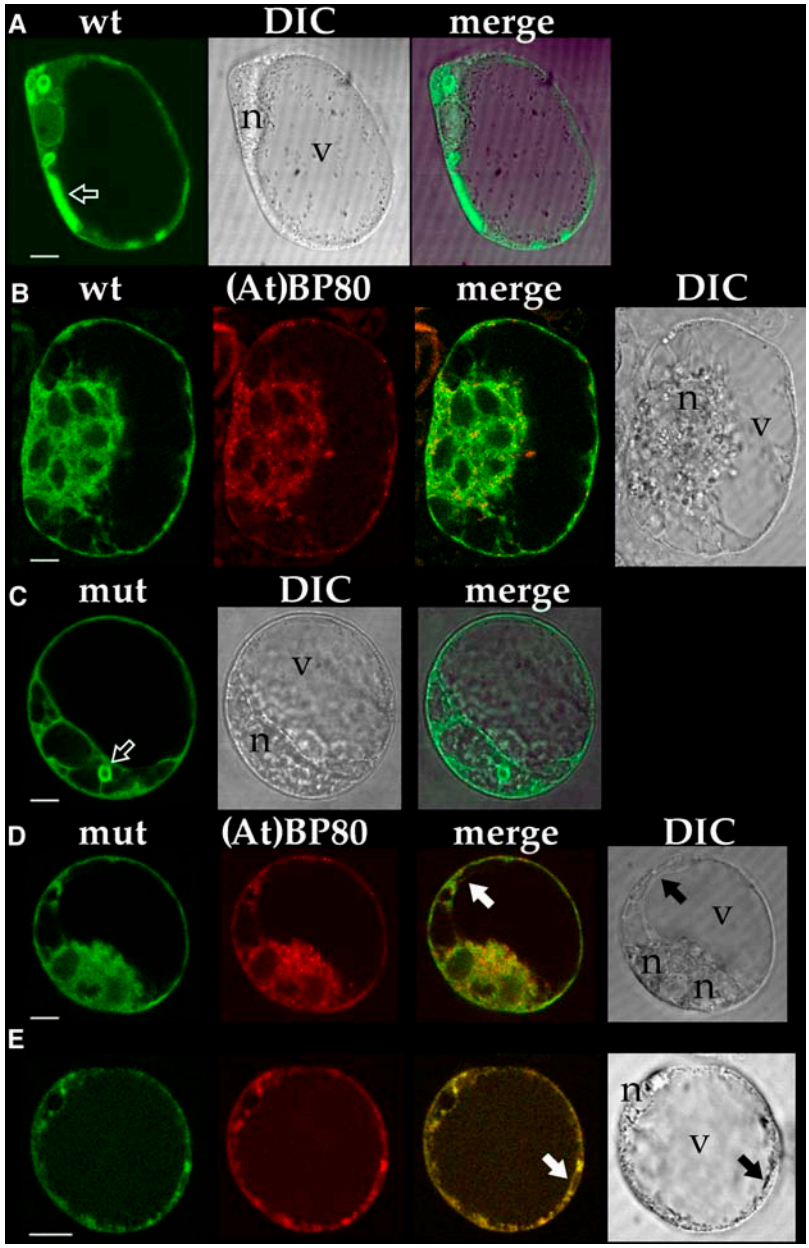

Figure 4. Expression of GFP-Tagged α-TIP and mRFP-Tagged Proaleurain-FLAG-(At)BP80b Transmembrane Domain and Cytoplasmic Tail [(At)BP80b-mRFP] Constructs in Protoplasts.

Cells were studied 16 to 20 h after electroporation. The images in line under each letter came from one cell; green indicates GFP, red indicates mRFP, merge indicates an image resulting from superimposition of the two images immediately to the left, and DIC (differential interference contrast) indicates a transmitted light image from that specific cell.

(A) Cell expressing GFPαTIP (wt); arrow indicates GFP-tagged structure that did not have a visible lumen when sequential optical sections were collected at 0.5-μm steps.

(B) Cell expressing GFPαTIP (wt) and (At)BP80b-mRFP. This cell has six nuclei, one of which is indicated with an ''n.''

(C) Cell expressing GFPαTIPΔ (mut, green); arrow indicates brightly labeled vacuole.

(D) and **(E)** Cells expressing GFPαTIPΔ (mut, green) and (At)BP80b-mRFP (red); arrows indicate central vacuole tonoplast tagged with GFP. n, position of nucleus; v, central vacuole.

a Ni^{2+}-agarose column, and incubated with either CPIEPPPHH (designated the specific peptide) or CHQPLATEDY (designated the nonspecific peptide) coupled to agarose beads via their N-terminal Cys residues. The presence of the proteins in unbound or drain fraction (D, Figure 5), the wash fraction (W, Figure 5), and the fraction eluted from the peptide-agarose resin with SDS (E, Figure 5) was determined by immunoblot assay. Figure 5A shows the results of an experiment where the proteins were incubated with the resin in the presence of 75 mM NaCl. Under these conditions, (At)VAP (right panel) appeared to bind only the specific peptide, and the recombinant protein was recovered only when eluted with SDS. When applied to the nonspecific peptide, no binding occurred and the protein was completely recovered in the drain fraction. By contrast, (At)SRC2 (left panel) showed a slightly different pattern. The protein fully bound the specific peptide and was exclusively recovered in the elution fraction. However, a considerable proportion of (At)SRC2 was also able to bind to the nonspecific peptide in 75 mM NaCl. When the binding assay was performed in the presence of increasing concentrations of NaCl (Figure 5B), binding to the nonspecific peptide was diminished such that no binding was observed in 250 mM NaCl, while interaction with the specific peptide was not affected by that salt concentration.

For in vitro assays of protein interactions, increasing Na concentration is a standard method to increase the stringency of protein–protein binding. We make no claims that this mimics the environment in the cell cytoplasm (where K is the predominant monovalent cation). Indeed, within the normal environment for (At)SRC2, it is likely that other proteins would participate in a complex that interacts with a target (e.g., PIEPPPHH), and we cannot replicate such a complex. The experiment simply demonstrates that, under conditions where the Na concentration requires higher affinity interactions, (At)SRC2 prefers to interact with PIEPPPHH. These results are consistent with the results obtained in the yeast two-hybrid screen and indicate that both (At)VAP and (At)SRC2 specifically interact with PIEPPPHH as compared with HQPLATEDY.

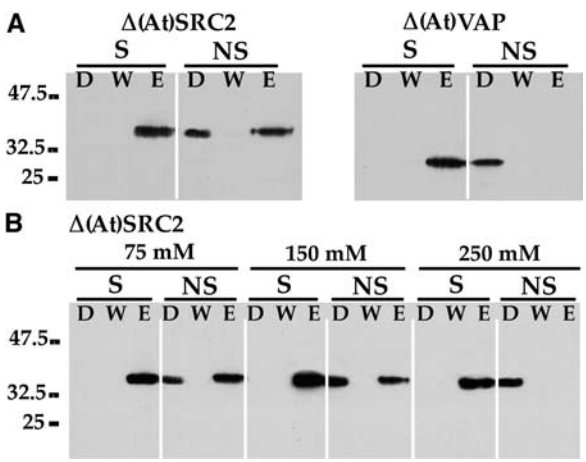

Figure 5. In Vitro Binding Assay.

Purified recombinant proteins lacking transmembrane and C-terminal lumenal sequences, designated Δ(At)SRC2 and Δ(At)VAP, were incubated with agarose-immobilized specific (S; CYPIEPPPHH) and nonspecific (NS; CHQPLATEDY) peptides. Unbound proteins were recovered in the drain (D) and the wash (W) steps. Bound proteins were eluted (E) with a 2% SDS buffer and detected on an immunoblot using their corresponding antibodies.

(A) The binding reaction was performed in the presence of 75 mM NaCl for both Δ(At)SRC2 and Δ(At)VAP.

(B) The binding specificity of Δ(At)SRC2 was tested in 75, 150, and 250 mM NaCl as indicated.

Immunolocalization of (At)SRC2 and (At)VAP

If (At)SRC2 and (At)VAP interact with the Re-F-B-α PIEPPPHH cytoplasmic sequence in vivo, we would expect to find that they colocalized with Re-F-B-α when coexpressed in cells. Therefore, tobacco protoplasts were cotransformed to express Re-F-B-α with (At)SRC2, Re-F-B-α with (At)VAP, or (At)SRC2 with (At)VAP. The protoplasts were fixed and the proteins were detected by immunofluorescence using their respective antibodies (Figure 6). The reporter protein Re-F-B-α was detected with antialeurain antibodies and, consistent with previous studies (Jiang and Rogers, 1998; Jiang et al., 2000) was present in numerous small punctate and round organelles distributed throughout the cytoplasm that are consistent with the size of PAC vesicles. (At)SRC2 and (At)VAP were detected with their respective antipeptide antibodies. When Re-F-B-α was coexpressed with (At)SRC2, antibody labeling showed essentially complete colocalization of the two proteins, as indicated by the yellow color in the merged panel (Figure 6A, arrow), indicating that these proteins were present on the same organelles. By contrast, when (At)VAP and Re-F-B-α were coexpressed (Figure 6B), essentially all organelles labeled for (At)VAP also labeled for Re-F-B-α, but larger organelles that usually surrounded nuclei appeared to contain only Re-F-B-α but not (At)VAP (arrowhead). No labeling above background with either antibody was observed in untransformed cells (data not shown), and similar results with transformed cells were obtained with both (At)SRC2 and (At)VAP antirecombinant protein antibodies (data not shown). Thus, both (At)SRC2 and (At)VAP were present in organelles containing Re-F-B-α, and, consistently, (At)VAP colocalized with (At)SRC2 on most of the labeled organelles except larger ones that typically were near the nucleus (Figure 6C, arrowhead).

Subcellular Localization of (At)SRC2 and (At)VAP Expressed in Tobacco Protoplasts

Previous studies demonstrated that the punctate and round organelles containing Re-F-B-α, PAC vesicles, and larger organelles on the PSV pathway were separate from ER and Golgi and partitioned with vacuoles during subcellular fractionation (Jiang and Rogers, 1998; Jiang et al., 2000). Therefore, one would expect that most of (At)SRC2 and (At)VAP would fractionate with a vacuolar fraction. We transformed tobacco suspension cell protoplasts with either (At)SRC2 or (At)VAP, separated cell vacuolar (Figure 7, V) and pellet (Figure 7, P) fractions, and analyzed their protein extracts on an immunoblot detected with antipeptide antibodies (Figure 7). (At)SRC2 fractionated such that ~10% was in the pellet fraction and ~90% was in the vacuole fraction

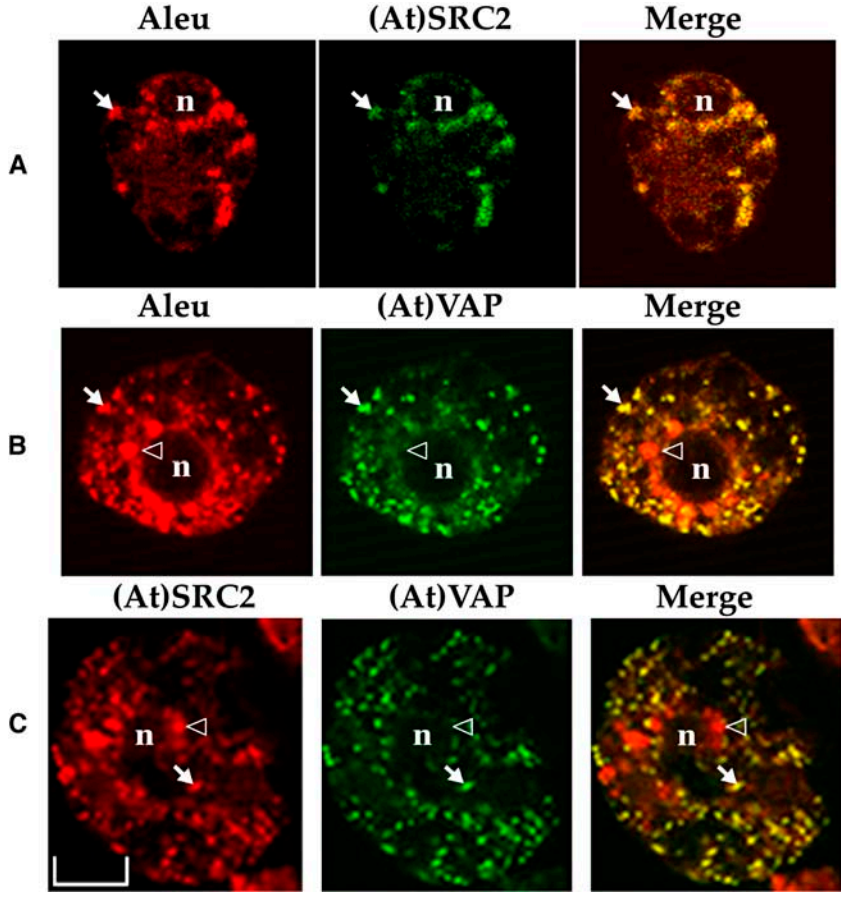

Figure 6. Confocal Immunolocalization of (At)SRC2, (At)VAP, and Re-F-B-α.

Tobacco protoplasts coexpressing Re-F-B-α with (At)SRC2 **(A)**, Re-F-B-α with (At)VAP **(B)**, or (At)SRC2 with (At)VAP **(C)** were fixed and incubated successively with antialeurain polyclonal antibodies (Aleu) and (At)SRC2 antipeptide antibodies **(A)**, antialeurain and (At)VAP antipeptide antibodies **(B)**, or (At)SRC2 antipeptide and (At)VAP antipeptide antibodies **(C)**. The first primary antibodies [Aleu and (At)SRC2; left column] were detected by anti-rabbit F(ab')$_2$-conjugated with lissamine rhodamine (red). The second primary antibodies [(At)SRC2 and (At)VAP; middle column] were detected using Alexa Fluor 488 anti-rabbit IgG (green). The yellow color on the merged panels (right column) indicates colocalization of green and red. Arrows, examples of colocalization of aleurain with (At)SRC2 **(A)**, aleurain with (At)VAP **(B)**, and (At)SRC2 with (At)VAP **(C)**; arrowheads, examples of regions where only aleurain **(B)** or (At)SRC2 **(C)** was detected; n, nucleus. Bar = 10 μm.

(Figure 7A, closed arrow). Bands indicated by the open arrows represent degradation products of the protein in both P and V fractions that were variably present in different experiments; they are not present in the nontransformed protoplasts (wild type). A cross-reacting endogenous protein (arrowhead) was present in both the transformed and the wild-type protoplasts. By contrast, (At)VAP protein exclusively partitioned in the vacuolar fraction (Figure 7B).

We next determined if (At)SRC2 and (At)VAP were exposed on the limiting membranes of the organelles to which they traffic. Vacuolar fractions isolated from transformed protoplasts were subjected to proteinase K digestion (Kirsch et al., 1994; Figure 8A). This step results in the proteolytic removal of polypeptides that are exposed on the cytoplasmic face of organelles. Proteins on immunoblots were detected with antirecombinant protein antibodies. (At)SRC2 was fully protected from protease digestion (Figure 8A, lane 5, closed arrow). Two cross-reacting endogenous proteins (open arrows), ~35 and ~90 kD, behaved differently and provided controls for the experiment. Similar to (At)SRC2, the ~35-kD protein was protease resistant, while, by contrast, the ~90-kD protein was protease sensitive and the corresponding band disappeared from samples treated with the protease (lanes 2 and 5). Treatment of the samples with Nonidet P-40 detergent solubilized membranes and verified activity of the protease; bands previously resistant to the protease (lanes 2 and 5) were completely digested in the presence of Nonidet P-40 (lanes 3 and 6). In the case of (At)VAP, almost all of the protein was protease sensitive (lane 11, closed arrow). Similarly, an endogenous doublet of ~40 kD (open arrow) was also largely protease sensitive.

Taken together with the predicted structures of the proteins, these results indicate that in the vacuolar organelles, (At)VAP is positioned on the limiting membrane such that, for most molecules, the long N-terminal region is accessible to protease

activity. By contrast, the cytoplasmic domain of (At)SRC2 was inaccessible to the protease, a result indicating either that the protein is internalized within the organelle or that the predicted type II orientation of (At)SRC2 is incorrect. We therefore compared the protease sensitivity of (At)SRC2 recovered in the nonvacuole pellet fraction to that in the vacuole fraction (Figure 8B). (At)SRC2 in the vacuole fraction (closed arrow; lanes 2 and 3) was completely resistant, while (At)SRC2 in the pellet fraction was fully accessible to the protease (lanes 5 and 6). In the panels below, control proteins were analyzed in aliquots from the same fractions used in the top panels. In the vacuole fraction, the 68-kD subunit A of the peripheral complex of vacuolar H^+-ATPase (Matsuura-Endo et al., 1990) was, as would be expected, completely digested by proteinase K. By contrast, in the pellet fraction, the lumenal ER chaperone BiP was completely protected from digestion. Thus, (At)SRC2 in membranes in the pellet fraction is exposed on the membrane surface and is accessible to protease. By contrast, in the vacuole fraction, (At)SRC2 has become inaccessible to the protease and presumably has been internalized. We hypothesized that protease-sensitive (At)SRC2 in the pellet fraction represented protein in the ER and that the protein became protease resistant in the process of moving to the vacuole fraction. However, the protein gel blot results would not exclude the possibility that protease-sensitive (At)SRC2 resulted from breakage of vacuoles during the cell fractionation process, allowing the fragmented vacuole membrane to centrifuge to the pellet.

This question was addressed by testing the protease sensitivity of newly synthesized (At)SRC2 in the pellet and vacuole fractions. Protoplasts were transformed to express either (At)SRC2 (Figure 8C, top) or the chimeric reporter protein Re-F-B-B that carries the BP-80 cytoplasmic tail and traffics to a lytic compartment (Figure 8C, bottom), labeled with [^{35}S]Met + Cys for 1 h, then separated into pellet and vacuole fractions. The

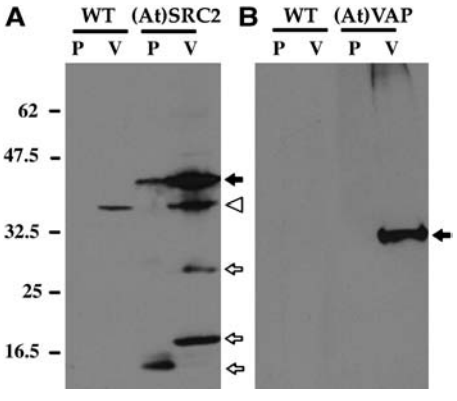

Figure 7. Subcellular Localization of (At)SRC2 and (At)VAP.

Nontransformed (WT) and (At)SRC2- or (At)VAP-transformed protoplasts were centrifuged onto a 15% Ficoll cushion. Intact vacuoles (V) were recovered from the top of the cushion and separated from the pellet (P). Solubilized proteins were analyzed on an immunoblot using anti-(At)SRC2 **(A)** or anti-(At)VAP **(B)** peptide antibodies. Closed arrows, positions of (At)SRC2 **(A)** and (At)VAP **(B)**; open arrows, degradation products of (At)SRC2; arrowhead, cross-reacting endogenous protein.

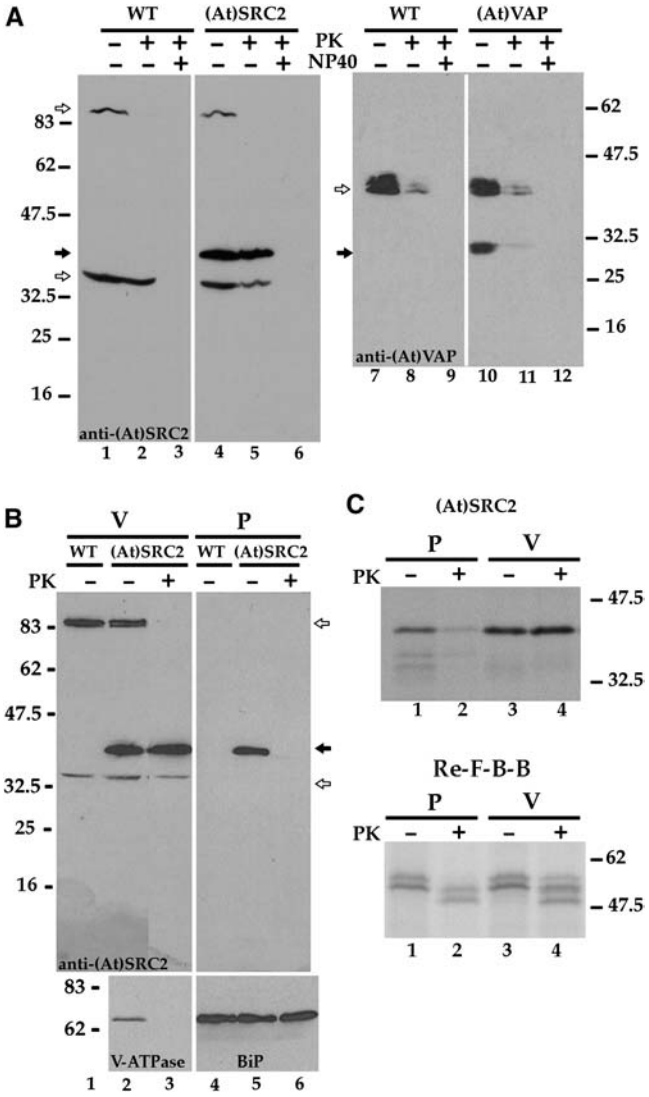

Figure 8. Proteinase K Protection Assay.

Nontransformed (WT) and (At)SRC2- or (At)VAP-transformed protoplasts were separated into vacuole (V) and pellet (P) fractions.

(A) Vacuoles were digested (+) or not digested (−) with proteinase K (PK) in the presence (+) or absence (−) of Nonidet P-40 (NP40) detergent. Proteins were detected on immunoblots using anti-(At)SRC2 or anti-(At)VAP recombinant protein antibodies.

(B) Vacuole and pellet fractions were separately treated (+) or not (−) with proteinase K and blotted for the detection of (At)SRC2 (top panel), subunit A of the peripheral complex of V-ATPase (bottom panel to the left), and BiP (bottom panel to the right). Closed and open arrows show the positions of (At)SRC2 or (At)VAP and cross-reacting endogenous proteins, respectively. Positions of molecular mass standards are indicated in kilodaltons at the side.

(C) Protoplasts transfected to express (At)SRC2 (top) or Re-F-B-B (bottom) were labeled with [^{35}S]Met + Cys for 1 h and then fractionated into pellet and vacuole fractions. Aliquots were separately treated (+) or not (−) with proteinase K, immunoprecipitated with anti-(At)SRC2 recombinant protein antibodies (top) or with anti-aleurain antibodies (bottom), and then separated by SDS-PAGE and visualized by fluorography.

fractions were treated with proteinase K, then (At)SRC2 and Re-F-B-B were immunoprecipitated and detected by fluorography. As judged from densitometry analyses of the fluorographs, without proteinase treatment, 37% of (At)SRC2 was recovered in the pellet and 63% was in the vacuole fraction. All protein (116%) in the vacuole fraction was recovered after proteinase treatment, but only 27% of the protein in the pellet fraction was proteinase resistant.

Analysis of proteinase resistance by Re-F-B-B served as a control. The full-length protein migrates as a doublet, due to different extents of glycosylation (Jiang and Rogers, 1998). After proteinase K treatment of the pellet fraction (lane 2), both bands of the doublet shifted to smaller size; the top band of the proteinase-treated doublet was slightly smaller in size than the bottom band of the control doublet (lane 1). This change in size was consistent with proteolytic removal of the cytoplasmic tail from both forms of the protein. We ask the reader to focus on the top band representing the most heavily glycosylated form of the protein because the amount of radioactivity in this band could be quantitated cleanly, separate from contamination by the lower band. All of this form of the protein in the pellet fraction and ~80% of it in the vacuole fraction was sensitive to proteinase digestion. Thus, the degree of proteinase resistance observed for (At)SRC2 in both pellet and vacuole fractions was not due to inadequate proteinase K activity, but rather represented protection of the protein from the proteinase.

The results indicate that (At)SRC2 moved quickly after synthesis to organelles that fractionate with vacuoles, presumably PAC vesicles, where it was fully protease resistant. By contrast, more than one-third of the newly synthesized protein remained in the pellet fraction where most of it was protease sensitive. This result argues that protein present at the site of synthesis in the ER accounts for the protease-sensitive fraction in the pellet. However, the exact site at which internalization of (At)SRC2 to protease-resistant form occurs, and the time after synthesis of an individual molecule required for internalization to occur remain to be determined by other experimental approaches.

We further tested the hypothesis that (At)SRC2 is internalized in vacuoles in two ways. First, we localized endogenous (At)SRC2 in PSVs in embryo cells from dry *Arabidopsis* seeds. As shown in Figure 9A, these PSVs are marked by the presence of α-TIP on their limiting membranes and by a granular-appearing network labeled by anti-DIP antibodies within. Anti-(At)SRC2 recombinant protein antibodies labeled internal structures with a similar appearance (Figure 9B). When double labeling was performed with either anti-(At)SRC2 recombinant protein antibodies (Figure 9C) or anti-(At)SRC2 peptide antibodies (Figure 9D) and anti-DIP antibodies, (At)SRC2 and DIP labeling colocalized. These immunofluorescence results are fully consistent with biochemical and immunolocalization studies demonstrating the presence of a crystalloid-like structure within PSVs of *Brassica napus* and *Arabidopsis* (Gillespie et al., 2005) and indicate that endogenous (At)SRC2 is internalized into membrane-containing structures similar to crystalloids in PSVs of *Arabidopsis*.

In a second approach, we determined the destination of (At)SRC2 and (At)VAP when expressed in transgenic tobacco seeds. Tobacco plants were stably transformed to express either (At)SRC2 or (At)VAP, expression was confirmed by immunoblot analysis of leaf extracts (data not shown), and seeds were harvested and processed for immunofluorescence studies. Seed sections from untransformed plants showed no labeling by the antibodies above background (data not shown). In transgenic seeds expressing (At)SRC2, anti-(At)SRC2 peptide antibodies labeled structures within PSVs and colocalized with anti-DIP antibodies (Figure 9E). This pattern of labeling is diagnostic of localization to the PSV crystalloid (Jiang et al., 2000). By contrast, transgenic seeds expressing (At)VAP showed labeling with anti-(At)VAP peptide antibodies around the periphery of PSVs, labeling that colocalized with anti-δ-TIP antibodies (Figure 9F). This labeling pattern is diagnostic of localization to the PSV tonoplast (Jiang et al., 2000, 2001). These results are consistent with results from the protease protection assays in protoplast transient expression experiments. (At)VAP was predominantly exposed on the limiting membranes in the protoplast vacuole fraction and was delivered to the limiting membrane of transgenic tobacco seed PSVs, while (At)SRC2 was internalized within the protoplast vacuole fraction and was delivered to crystalloids in transgenic tobacco seed PSVs.

DISCUSSION

Protein aggregates within the ER are transferred to lysosomes in mammalian cells (Noda and Farquhar, 1992). Thus, the concept of a direct ER-to-vacuole pathway extends beyond plant cells, but the process appears to be more prominent in the plant system. Organelles to which ER membrane and proteins are transferred as an intermediate step to PSVs, PAC vesicles, have been identified both in developing seeds (Hara-Nishimura et al., 1998; Jiang et al., 2000) and in root tip cells (Jiang et al., 2000). It therefore is likely that the mechanisms for ER-to-vacuole transfer function in many different plant cell types.

PAC vesicle budding is thought to occur at ER loci where intralumenal inclusions are present (Hara-Nishimura et al., 1998). In some cases, formation of abnormal storage protein aggregates in transgenic plants is followed by their budding into cytoplasmic vesicles (Hayashi et al., 1999; Kinney et al., 2001), although their transfer to PSVs was not observed in soybean embryos (Kinney et al., 2001). A similar process may normally occur for the transfer of prolamin protein bodies from ER to vacuoles in developing wheat seeds (Levanony et al., 1992). In other cases, the origin of ER inclusions is unexplained, but one possible clue has come from studies in *Arabidopsis*. It was noted that signal peptide GFP carrying a C-terminal HDEL for ER retention was concentrated in spindle-shaped, mobile structures (Gunning, 1998; Hawes et al., 2001). These ER bodies are stress induced (Matsushima et al., 2002) and contain a β-glucosidase with a C-terminal KDEL (Matsushima et al., 2003) and two stress-inducible Cys proteases (Hayashi et al., 2001). Thus, structures with a selected lumenal protein content can form at discrete loci in the ER, and it is possible that these loci are the sites from which PAC vesicles bud. This hypothesis requires the sites of PAC vesicle formation to represent a distinct subdomain of the ER where specific membrane proteins and lumenal contents have been selected and enriched. The precedent for functionally distinct ER subdomains in plant cells is well established (Staehelin, 1997).

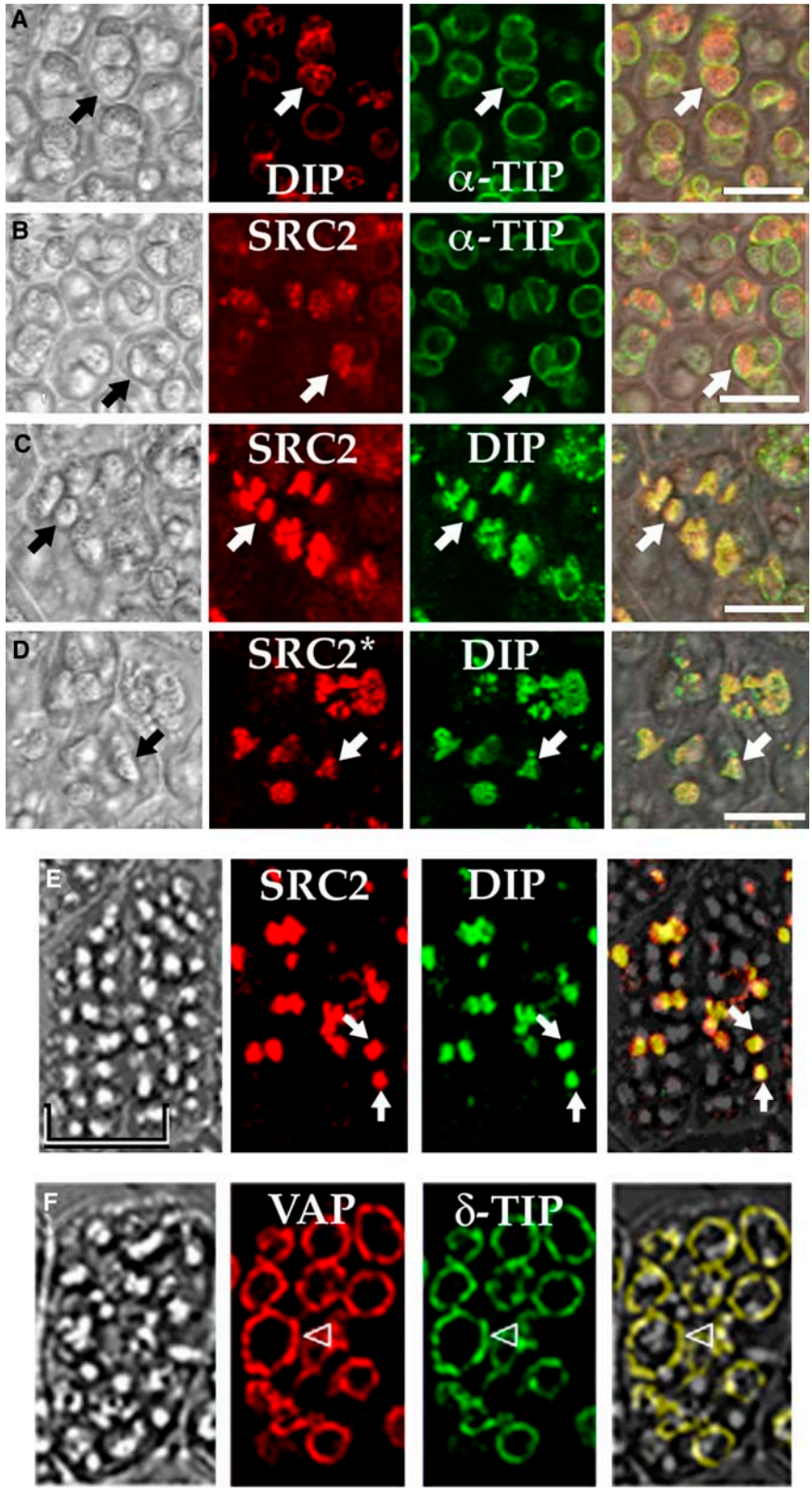

Figure 9. (At)SRC2 Is Internalized within Vacuoles.

(A) to **(D)** Immunolocalization in embryo cells in mature, dry *Arabidopsis* seeds. Sections were labeled with the combinations of antibodies indicated;

In this regard, the finding that (At)SRC2 rapidly moves after synthesis from ER to a vacuole fraction where it is has been internalized may be notable. Structural features of (At)SRC2 may help explain its possible role in PSV targeting and the associated membrane internalization. First, the lumenal domain sequences of (At)SRC2 homologs from different plant species are highly conserved and terminate in GGFDF. These domains have a striking pattern of multiple Asp residues alternating regularly with Gly and hydrophobic residues. In addition, the *Saccharomyces cerevisiae* YFL010c protein represents essentially an SRC2 protein lacking the N-terminal C2 domain and has similar characteristics in its lumenal region. In all sequences, the concentration of acidic Asp residues might serve as a focus for coordination of Ca^{2+} ions. Perhaps the lumenal domain localizes (At)SRC2 to the sites at which a specific lumenal protein complex assembles. The second structural feature that is likely to play an important role in the protein's function is the N-terminal C2 domain. The C2 domain's ability to interact with phospholipids (Rizo and Südhof, 1998) could help link (At)SRC2 to a second membrane, perhaps as a step leading to membrane folding and internalization.

A third structural feature, the ability of (At)SRC2 to interact with the ER-to-vacuole targeting signal, PIEPPPHH, coupled with the colocalization of (At)SRC2 and the Re-F-B-α reporter protein on small organelles that fractionate with vacuoles in our transient expression system, may indicate a role for (At)SRC2 in traffic of Re-F-B-α in that pathway. Our data regarding the targeting of GFPαTIP indicate that PIEPPPHH also plays an important role in targeting intact α-TIP to its vacuole destination and support the concept that most α-TIP, similar to Re-F-B-α, does not traffic through the Golgi. This concept is consistent with a recent study that reported the movement of full-length α-TIP to small vacuoles separate from central vacuoles in leaf cells of tobacco, common bean, and *Arabidopsis* (Park et al., 2004). Movement to the small vacuoles from ER was not sensitive to treatment with brefeldin A, was not prevented by a dominant negative mutant of AtRab1, and was not prevented by overexpression of AtSec23. By contrast, all three manipulations blocked traffic of the bean storage protein phaseolin to vacuoles, movement that is known to involve traffic through the Golgi apparatus. The authors concluded that the movement of α-TIP to PSVs utilizes a Golgi-independent pathway (Park et al., 2004).

How can this assertion be reconciled with results from immunoelectron microscopy studies where antiserum to α-TIP labeled Golgi and dense vesicles that carry storage proteins from Golgi to the PSV (Hinz et al., 1999; Hillmer et al., 2001; Jolliffe et al., 2004)? These studies used crude antiserum raised to a protein band excised from an SDS-PAGE gel where membrane proteins from bean PSVs were separated; it was stated that N-terminal sequencing demonstrated only the predicted sequence from α-TIP (Johnson et al., 1989), but this result would not exclude the presence of other proteins with blocked N termini. Subsequent studies of PSV TIPs showed that the tonoplast of PSVs from seeds carried both α- and δ-TIPs, and the sizes of the two proteins were very similar (Jauh et al., 1999) such that the gel conditions used (Johnson et al., 1989) probably would not have separated them. When SDS-PAGE separation of membrane proteins from pea (*Pisum sativum*) seeds was performed using

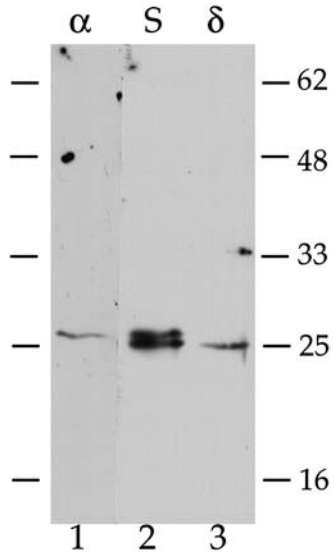

Figure 10. Immunoblot Analyses of TIPs in Pea Seed Membrane Proteins.

Protein extracts from dry, mature pea seeds were prepared as described (Jauh et al., 1999). Three 50-μg samples were electrophoresed through a 15% acrylamide SDS-PAGE gel, where molecular mass markers bracketed either side. After transfer to nitrocellulose, the membrane was stained with Ponceau red to identify the lanes. Three strips were excised, where notches at the bottom were placed to allow exact alignment of the strips: strip 1 (α), markers + pea proteins, incubated with isoform-specific anti-α-TIP peptide antibodies (Jauh, et al., 1999), 1 μg/mL; strip 2 (S), pea proteins, incubated with anti-α-TIP antiserum (Johnson et al., 1989), 1:2000; strip 3 (δ), pea proteins plus markers, incubated with isoform-specific anti-δ-TIP peptide antibodies, 10 μg/mL. After overnight incubation, the strips were processed for detection by chemiluminescence. The exposures presented are 10 s for strip 1 and 2 s for strips 2 and 3. Bars to either side indicate positions of molecular mass markers in kilodaltons.

Figure 9. (continued).

SRC2 indicates anti-SRC2 recombinant protein antibody, while SRC2* indicates anti-SRC2 peptide antibody. Arrows indicate examples of PSVs within each set of images. Bars = 10 μm.

(E) and **(F)** Sections of mature seeds from transgenic tobacco plants expressing (At)SRC2 **(E)** or (At)VAP **(F)** were labeled with polyclonal antibodies against either (At)SRC2 and DIP **(E)** or (At)VAP and δ-TIP **(F)**. Arrows, examples of colocalization of (At)SRC2 with DIP; arrowheads, colocalization of (At)VAP with δ-TIP. Bar = 10 μm for **(E)** and **(F)**.

In each case, sections labeled with each antibody individually gave the same pattern as shown for that antibody in the double label images (data not shown). To the left for each set of panels is the transmitted light image, while the panel at the right represents the transmitted light plus red plus green images superimposed. Colocalization of the antibodies is indicated by yellow color.

a higher acrylamide concentration, the anti-α-TIP antiserum detected two closely spaced bands, where the upper band corresponds to the protein detected by the isoform-specific anti-α-TIP peptide antibodies, and the lower band corresponds to the protein detected by isoform-specific anti-δ-TIP peptide antibodies (Figure 10). Similar results were previously obtained in David Robinson's laboratory (A. Olbrich and D.G. Robinson, personal communication). Thus, the possibility exists that studies using this antiserum where Golgi labeling was obtained might have detected δ-TIP rather than α-TIP.

However, alternatively, perhaps traffic of α-TIP is specifically associated with membrane incorporated into vesicles that transport storage protein aggregates to the PSV. Because storage protein aggregation occurs in different organelles in different cell types (Okita and Rogers, 1996), α-TIP could variably exit either the ER or the Golgi in transit to the PSV. We think this explanation is less likely because our studies of Re-F-B-α and of α-TIP traffic utilized protoplasts where storage protein aggregation was not known to be present. Nevertheless, whether (At)SRC2 could also function at the level of the Golgi under some circumstances is not known.

These considerations, however, emphasize that traffic of TIPs likely reflects the need for plant cells to define specific types of membrane and to control membrane traffic carefully because only with such control could functionally distinct vacuolar compartments be generated and maintained (Okita and Rogers, 1996; Jauh et al., 1999). The ER-to-PSV traffic defined by α-TIP and by (At)SRC2 in our protoplast system may represent a crucial mechanism for biogenesis of not only the PSV limiting membrane but also for internalized membranes that ultimately form the PSV crystalloid.

METHODS

Yeast Two-Hybrid Screening

The Matchmaker Two-Hybrid System 3 was obtained from BD Biosciences Clontech, and experimental procedures were done according to its protocols. Three tandemly repeated units of the functionally defined residues, PIEPPPHH, were fused to the DNA binding domain of the bait plasmid. The coding sequence was created by annealing the complementary oligonucleotides MO962639 (5′-CGCGGATCCCCAATTGAACCACCCCCACACCACCCAATTGAACCACCCCCACACCACCCAATTGAACCACCCCCACACCACCTGCAGTTT-3′), corresponding to the sense strand carrying a *Bam*HI site at the 5′ region, and MO962640 (5′-AAACTGCAGGTGGTGTGGGGGTGGTTCAATTGGGTGGTGTGGGGGTGGTTCAATTGGGTGGTGTGGGGGTGGTTCAATTGGGGATCCGCG-3′), corresponding to the antisense strand containing a *Pst*I site at the 5′ region. The double-stranded DNA fragment was then digested with *Bam*HI and *Pst*I endonucleases and ligated into the multiple cloning site of the bait plasmid (pGBKT7 of the Matchmaker 3 kit). The resulting fusion protein was used to screen an *Arabidopsis thaliana* vegetative tissue cDNA library in plasmid pGAD10, also purchased from Clontech, for potential PIEPPPHH binding proteins.

Cloning of Full-Length and C-Terminal Truncated (At)SRC2 and (At)VAP

Expressed sequence tag clones 204L3T7 and 211P17T7, corresponding to (At)SRC2 and (At)VAP, respectively, were kindly provided by the Arabidopsis Biological Resource Center at Ohio State University. Full-length (At)SRC2 and (At)VAP coding sequences were amplified from the cDNAs using the following oligonucleotides: MO1553142 (5′-GGGGATCCGCAAATTTCAAGTTTATTTCA-3′) and MO1553144 (5′-GGGAGCTCAGTGGTGGTGGTGGTGGTGGAAATCGAAACCACCCATGTC-3′) for (At)SRC2, and MO1553145 (5′-GGGGATCCCGATCGACGACTGCTCTCTCT-3′) and MO1553147 (5′-GGGAGCTCAGTGGTGGTGGTGGTGGTGTCCTCTTCATAATGTATCC-3′) for (At)VAP. Note that all of the four 3′ oligonucleotides, MO1553144, MO1553147, MO1553143, and MO1553146, contain a sequence coding for six His residues (underlined above), allowing the products to carry a His-tag at their C termini. The following oligonucleotides were used to prepare coding sequences for truncated proteins lacking transmembrane domains: MO1553143 (5′-GGGAGCTCAGTGGTGGTGGTGGTGGTGCTTACCATGCTTCTTCGGTTTC-3′) for Δ(At)SRC2 and MO1553146 (5′-GGGAGCTCAGTGGTGGTGGTGGTGACTTTGGCTCTTTTTGCTTTC-3′) for Δ(At)VAP. For expression in plant cells, the four amplified DNA sequences were each inserted between *Bam*HI and *Sac*I sites of the plasmid LJ526 (Jiang and Rogers, 1998).

Preparation of GFP-αTIP and GFP-αTIPΔ

Enhanced GFP cDNA was obtained from BD Biosciences Clontech. The *Phaseolus vulgaris* α-TIP cDNA (GenBank accession number X62873) was generously provided by Maarten Chrispeels (University of California, San Diego, CA). PCR products were generated with appropriate oligonucleotide primers to yield the following DNA fragments with flanking restriction enzyme sites: *Bam*HI-enhanced GFP–*Xho*I; *Xho*I–α-TIP–*Sac*I; *Xho*I–α-TIP with PIEPPPHH deleted–*Sac*I. The sequence of the oligonucleotide primer used to generate the deletion was 5′-CCGAGCTCTAGTAATCTTCAGTTGCCAAAGGTTGGATCACAGCATATTCATA-3′. The fragments were inserted sequentially as *Bam*HI-*Xho*I and *Xho*I-*Sac*I fragments into the appropriate intervals of LJ526 (Jiang and Rogers, 1998) to yield in-frame fusions flanked by the cauliflower mosaic virus 35S promoter and the nopaline synthase poly(A) addition sequence.

Preparation of the Proaleurain-FLAG-AtBP80 Transmembrane and Cytoplasmic Tail Expression Construct Carrying mRFP Inserted in the Cytoplasmic Tail: AtBP80-mRFP

The template for PCR amplification was the VSR_{At1} cDNA (GenBank accession number U79959). The 5′ oligonucleotide placed an *Eco*RI site preceding nucleotide 1841: 5′-GGGAATTCGGCAAAGTTGGAACCACAAAAC-3′. The 3′ oligonucleotide changed the coding sequence for the final two amino acids to insert a *Bgl*II site immediately before the stop codon: 5′-CAAGTGGTCACCATATGAGATCTTGAGCTCCC-3′. The resulting DNA fragment was substituted for the *Eco*RI-*Sac*I fragment of LJ526. The mRFP cDNA was generously supplied by Roger Tsien (University of California, San Diego) (Campbell et al., 2002). This sequence was amplified to place a *Bgl*II site at the 5′ end and a *Bam*HI site at the 3′ end: 5′ oligonucleotide, 5′-GGAGATCTATGGCCTCCTCCGAGGACGT-3′; 3′ oligonucleotide, 5′-CCGGATCCGGCGCCGGTGGAGTGGCG-3′.

The resulting DNA fragment was inserted into the *Bgl*II site of the modified VSR_{At1} cytoplasmic tail, proper orientation was determined by digestion with *Bgl*II and *Sac*I, and the complete construct was designated JR900.

Protoplast Transient Expression, Preparation of Vacuole and Pellet Membrane Fractions, Immunoblot Analysis, Immunoprecipitation, and Immunofluorescence

These techniques were performed as previously described using protoplasts from TxD tobacco (*Nicotiana tabacum*) suspension culture cells (Jiang and Rogers, 1998) with the following modifications. For SDS-PAGE analysis of Re-F-B-α recovered in vacuole and pellet fractions, it was first

necessary to remove excess lipid by precipitating the proteins from SDS-PAGE sample buffer with 10 volumes of acetone. The acetone pellet was then resuspended in SDS-PAGE sample buffer for electrophoresis. For immunofluorescence double labeling, the first primary antibody was detected with anti-rabbit $F(ab')_2$ fragments conjugated with lissamine rhodamine (Jackson Immunoresearch Laboratories). The second primary antibody was detected using Alexa Fluor 488 anti-rabbit IgG (Molecular Probes). Fluorescence-labeled protoplasts were examined by laser scanning confocal microscopy with an inverted compound microscope (Nikon model TE300), using a Planado ×60 oil immersion objective. Fluorescence images were collected using a Bio-Rad MRC 1024 system with a laser level of 3% and an iris setting of 2. Images were processed in an identical manner using Adobe Photoshop software. Controls accompanied all double-labeling experiments as described (Jiang et al., 2000, 2001; Jiang and Rogers, 1998). For protoplasts expressing GFP fusion proteins, 20 μL of protoplast suspension at room temperature was diluted into an equal volume of 37°C 2% low melting point agarose (Sigma-Aldrich) in TxD suspension culture cell medium containing 0.2 M mannitol, and 20 μL was placed in a large circle drawn with a wax pencil on a microscope slide and then covered with a cover slip and sealed with clear nail polish. Slides were scanned using wide-field epifluorescence to identify cells expressing the fusion proteins, and then transfected protoplasts were imaged by laser scanning confocal microscopy using the Bio-Rad MRC 1024 system with 30% laser power and the Planado ×60 oil immersion objective. For each cell, at least two optical sections were collected at 5-μm steps beginning at the level of the nucleus. Excitation was provided by a krypton/argon laser at 488 and 568 nm; emission filters were a 585-nm EFLP filter for photomultiplier tube 1 (red), and a 522-nm DF32 filter with a 560 DF block for photomultiplier tube 2 (green). Iris settings of 3.0 were used for both channels.

Preparation of Anti-(At)SRC2 and Anti-(At)VAP Antibodies

Two sets of polyclonal antibodies were prepared for each of the two proteins. Antirecombinant protein antibodies were prepared against the first 160 amino acids of (At)VAP and the region lying between amino acids 87 and 166 of (At)SRC2. Specific antipeptide antibodies were raised against the following synthetic peptides: 266-QAHGKPQKPKKHGK-279 for (At)SRC2 and 179-FIVDNKAGHQENT-191 for (At)VAP. The procedures followed were as described previously (Jauh et al., 1999). Affinity-purified antibodies (Holwerda et al., 1990; Kirsch et al., 1994) were used in all experiments. Before use in immunofluorescence experiments, antibodies were absorbed with acetone powder prepared from TxD suspension culture cells (Jiang et al., 2001) to remove cross-reactivity with endogenous tobacco proteins.

In Vitro Binding Assay

Truncated (At)SRC2 [Δ(At)SRC2] and (At)VAP [Δ(At)VAP], lacking transmembrane and lumenal sequences but carrying six His residues at their C termini, were expressed in tobacco protoplasts. Cells were lysed in 6 M guanidine HCl, 100 mM $NaPO_4$, and 10 mM Tris-HCl, pH 8.0, with continuous mixing for 1 h at room temperature, then centrifuged at 10,000*g* for 15 min. Four hundred microliters of a 50% slurry of Ni^{2+}-agarose (Qiagen) was added to the supernatants and incubated for 1 h with continuous mixing. Ni^{2+}-agarose beads were collected by centrifugation for 2 min at 1000*g* and washed with 8 M urea, 100 mM $NaPO_4$, and 10 mM Tris-HCl, pH 8.0. Ni^{2+}-agarose–bound recombinant proteins were eluted with 800 μL of 200 mM imidazole, pH 7.7, and dialyzed against 50 μM $CaCl_2$, 1 mM DTT, 75 mM NaCl, and 20 mM Tris-HCl, pH 7.2. Specific (CYPIEPPPHH) and nonspecific (CHQPLATEDY) peptides were coupled to agarose beads using SulfoLink coupling gel (Pierce). Purified Δ(At)SRC2 and Δ(At)VAP were separately incubated with agarose-bound specific and nonspecific peptides for 2 h in 50 μM $CaCl_2$, 1 mM $MgCl_2$, 1 mM DTT, 20 mM Tris-HCl, pH 7.2, and either 75, 150, or 250 mM NaCl. Unbound proteins were collected, the beads were washed with fresh binding buffer, and bound proteins were eluted with a 2% SDS buffer. Fractions were analyzed for the presence of Δ(At)SRC2 and Δ(At)VAP on an immunoblot using their respective antibodies.

Proteinase K Digestion Assay

Untransformed and (At)SRC2- and (At)VAP-transformed protoplasts were centrifuged onto a 15% Ficoll layer overlaying a 68% sucrose cushion (Holwerda et al., 1990; Jiang and Rogers, 1998). Vacuole and pellet fractions were recovered from the top of the Ficoll and the interface between Ficoll/sucrose, respectively. Proteinase K (Roche Diagnostics) was dissolved at 10 mg/mL in 0.5 mM $MgCl_2$, 1 mM EGTA, and 100 mM MES buffer, pH 6.5, and stored in aliquots at −80°C until use. Proteins exposed to the cytoplasm were digested for 1 h in the proteinase K storage buffer containing 200 mM mannitol and 10 μg/mL Proteinase K. Control samples were digested in the presence of 1% Nonidet P-40 to remove membrane barriers. Reactions were terminated by addition of phenylmethylsulfonyl fluoride to 2 mM. Proteins were precipitated in 5% trichloroacetic acid, the precipitate was washed with acetone and resuspended in SDS-PAGE sample buffer, and (At)SRC2 and (At)VAP were detected on immunoblots using their respective antirecombinant protein antibodies. The lumenal ER chaperone BiP (antibodies generously provided by Alessandro Vitale, Istituto Biosintesi Vegetali, Milan, Italy) and subunit A of the peripheral complex of the vacuolar ATPase (antibodies generously provided by Masayoshi Maeshima, Nagoya University, Japan) served as controls.

Transgenic Tobacco Seeds

Tobacco plants expressing either (At)SRC2 or (At)VAP were generated using *Agrobacterium tumefaciens*–mediated transformation as previously described (Oufattole et al., 2000). Transgenic seeds were fixed in 3.7% paraformaldehyde, embedded, and processed as described (Jauh et al., 1999).

Accession Numbers

Sequence data from this article can be found in the GenBank/EMBL data libraries under accession numbers At1g09070 and At3g60600.

ACKNOWLEDGMENTS

This research was supported by grants MCB-9974429 from the National Science Foundation and RG0018/2000 from the Human Frontier Science Program. L.J. is supported by a grant from the Research Grants Council of Hong Kong (CUHK4156/01M). A portion of this work has been presented in abstract form (http://abstracts.aspb.org/pb2003/public/P69/1151.html). We thank Jack Widholm (University of Illinois, Urbana, IL) for assistance in reestablishing our TxD suspension culture cell line.

Received June 14, 2005; revised June 14, 2005; accepted September 12, 2005; published October 14, 2005.

REFERENCES

Campbell, R.E., Tour, O., Palmer, A.E., Steinbach, P.A., Baird, G.S., Zacharias, D.A., and Tsien, R.Y. (2002). A monomeric red fluorescent protein. Proc. Natl. Acad. Sci. USA **99,** 7877–7882.

Di Sansebastiano, G.P., Paris, N., Marc-Martin, S., and Neuhaus, J.-M. (1998). Specific accumulation of GFP in a non-acidic vacuolar compartment via a C-terminal propeptide-mediated sorting pathway. Plant J. **15,** 449–457.

Di Sansebastiano, G.P., Paris, N., Marc-Martin, S., and Neuhaus, J.-M. (2001). Regeneration of a lytic central vacuole and of neutral peripheral vacuoles can be visualized by green fluorescent proteins targeted to either type of vacuoles. Plant Physiol. **126,** 78–86.

Gillespie, J.E., Rogers, S.W., Deery, M., Dupree, P., and Rogers, J.C. (2005). A unique family of proteins associated with internalized membranes in protein storage vacuoles of the Brassicaceae. Plant J. **41,** 429–441.

Gunning, B.E.S. (1998). The identity of mystery organelles in *Arabidopsis* plants expressing GFP. Trends Plant Sci. **3,** 417.

Hadlington, J.L., and Denecke, J. (2000). Sorting of soluble proteins in the secretory pathway of plants. Curr. Opin. Plant Biol. **3,** 461–469.

Hara-Nishimura, I., Shimada, T., Hatano, K., Takeuchi, Y., and Nishimura, M. (1998). Transport of storage proteins to protein storage vacuoles is mediated by large precursor-accumulating vesicles. Plant Cell **10,** 825–836.

Hawes, C., Saint-Jore, C., Martin, B., and Zheng, H.-Q. (2001). ER confirmed as the location of mystery organelles in *Arabidopsis* plants expressing GFP! Trends Plant Sci. **6,** 245–246.

Hayashi, M., Toriyama, K., Kondo, M., Hara-Nishimura, I., and Nishimura, M. (1999). Accumulation of a fusion protein containing 2S albumin induces novel vesicles in vegetative cells of Arabidopsis. Plant Cell Physiol. **40,** 263–272.

Hayashi, Y., Yamada, K., Shimada, T., Matsushima, R., Nishizawa, H.K., Nishimura, M., and Hara-Nishimura, I. (2001). A proteinase-storing body that prepares for cell death or stresses in the epidermal cells of Arabidopsis. Plant Cell Physiol. **42,** 894–899.

Herman, E., and Schmidt, M. (2004). Endoplasmic reticulum to vacuole trafficking of endoplasmic reticulum bodies provides an alternate pathway for protein transfer to the vacuole. Plant Physiol. **136,** 3440–3446.

Hillmer, S., Movafeghi, A., Robinson, D.G., and Hinz, G. (2001). Vacuolar storage proteins are sorted in the cis-cisternae of the pea cotyledon Golgi apparatus. J. Cell Biol. **152,** 41–50.

Hinz, G., Hillmer, S., Bäumer, M., and Hohl, I. (1999). Vacuolar storage proteins and the putative sorting receptor BP-80 exit the Golgi apparatus of developing pea cotyledons in different transport vesicles. Plant Cell **11,** 1509–1524.

Hoh, B., Hinz, G., Jeong, B.-K., and Robinson, D.G. (1995). Protein storage vacuoles form de novo during pea cotyledon development. J. Cell Sci. **108,** 299–310.

Holwerda, B.C., Galvin, N.J., Baranski, T.J., and Rogers, J.C. (1990). In vitro processing of aleurain, a barley vacuolar thiol protease. Plant Cell **2,** 1091–1106.

Inoue, K., Motozaki, A., Takeuchi, Y., Nishimura, M., and Hara-Nishimura, K. (1995). Molecular characterization of proteins in protein-body membrane that disappear most rapidly during transformation of protein bodies into vacuoles. Plant J. **7,** 235–243.

Jauh, G.-Y., Fischer, A.M., Grimes, H.D., Ryan, C.A., and Rogers, J.C. (1998). δ-Tonoplast intrinsic protein defines unique plant vacuole functions. Proc. Natl. Acad. Sci. USA **95,** 12995–12999.

Jauh, G.-Y., Phillips, T., and Rogers, J.C. (1999). Tonoplast intrinsic protein isoforms as markers for vacuole functions. Plant Cell **11,** 1867–1882.

Jiang, L., Phillips, T.E., Hamm, C.A., Drozdowicz, Y.M., Rea, P.A., Maeshima, M., Rogers, S.W., and Rogers, J.C. (2001). The protein storage vacuole: A unique compound organelle. J. Cell Biol. **155,** 991–1002.

Jiang, L., Phillips, T.E., Rogers, S.W., and Rogers, J.C. (2000). Biogenesis of the protein storage vacuole crystalloid. J. Cell Biol. **150,** 755–769.

Jiang, L., and Rogers, J.C. (1998). Integral membrane protein sorting to vacuoles in plant cells: Evidence for two pathways. J. Cell Biol. **143,** 1183–1199.

Jiang, L., and Rogers, J.C. (1999). Functional analysis of a Golgi-localized Kex2p-like protease in tobacco suspension culture cells. Plant J. **18,** 23–32.

Johnson, K.D., Herman, E.M., and Chrispeels, M.J. (1989). An abundant, highly conserved tonoplast protein in seeds. Plant Physiol. **91**, 1006–1013.

Jolliffe, N.A., Brown, J.C., Neumann, U., Vicre, M., Bachi, A., Hawes, C., Ceriotti, A., Roberts, L.M., and Frigerio, L. (2004). Transport of ricin and 2S albumin precursors to the storage vacuoles of *Ricinum communis* endosperm involves the Golgi and VSR-like receptors. Plant J. **39,** 821–833.

Kim, W.T., Franceschi, V.R., Krishnan, H.B., and Okita, T.W. (1988). Formation of wheat protein bodies: Involvement of the Golgi apparatus in gliadin transport. Planta **173,** 173–182.

Kinney, A.J., Jung, R., and Herman, E.M. (2001). Cosuppression of the α subunits of β-conglycinin in transgenic soybean seeds induces the formation of endoplasmic reticulum-derived protein bodies. Plant Cell **13,** 1165–1178.

Kirsch, T., Paris, N., Butler, J.M., Beevers, L., and Rogers, J.C. (1994). Purification and initial characterization of a potential plant vacuolar targeting receptor. Proc. Natl. Acad. Sci. USA **91,** 3403–3407.

Laurent, F., Labesse, G., and Wit, P. (2000). Molecular cloning and partial characterization of a plant VAP33 homologue with a major sperm protein domain. Biochem. Biophys. Res. Commun. **270,** 286–292.

Levanony, H., Rubin, R., Altschuler, Y., and Galili, G. (1992). Evidence for a novel route of wheat storage proteins to vacuoles. J. Cell Biol. **119,** 1117–1128.

Li, Y.-B., Rogers, S.W., Tse, Y.C., Lo, S.W., Sun, S.S.M., Jauh, G.-Y., and Jiang, L. (2002). BP-80 and homologs are concentrated on post-Golgi, probable lytic prevacuolar compartments. Plant Cell Physiol. **43,** 726–742.

Lott, J.N.A. (1980). Protein bodies. In The Biochemistry of Plants, N.E. Tolbert, ed (New York: Academic Press), pp. 589–623.

Luban, J., and Goff, S.P. (1995). The yeast two-hybrid system for studying protein interactions. Curr. Opin. Biotechnol. **6,** 59–64.

Matsushima, R., Hayashi, Y., Kondo, M., Shimada, T., Nishimura, M., and Hara-Nishimura, I. (2002). An endoplasmic reticulum-derived structure that is induced under stress conditions in *Arabidopsis.* Plant Physiol. **130,** 1807–1814.

Matsushima, R., Kondo, M., Nishimura, M., and Hara-Nishimura, I. (2003). A novel ER-derived compartment, the ER body, selectively accumulates a β-glucosidase with an ER-retention signal in *Arabidopsis.* Plant J. **33,** 493–502.

Matsuura-Endo, C., Maeshima, M., and Yoshida, S. (1990). Subunit composition of vacuolar membrane H^+-ATPase from mung bean. Eur. J. Biochem. **187,** 745–751.

Mitsuhashi, N., Hayashi, Y., Koumoto, Y., Shimada, T., Fukasawa-Akada, T., Nishimura, M., and Hara-Nishimura, I. (2001). A novel membrane protein that is transported to protein-storage vacuoles via precursor-accumulating vesicles. Plant Cell **13,** 2361–2372.

Noda, T., and Farquhar, M.G. (1992). A non-autophagic pathway for diversion of ER secretory proteins to lysosomes. J. Cell Biol. **119,** 85–97.

Okita, T.W., and Rogers, J.C. (1996). Compartmentation of proteins in the endomembrane system of plant cells. Annu. Rev. Plant Physiol. Plant Mol. Biol. **47,** 327–350.

Oufattole, M., Arango, M., and Boutry, M. (2000). Identification and expression of three new *Nicotiana plumbaginifolia* genes which encode isoforms of a plasma-membrane H^+-ATPase, and one of which is induced by mechanical stress. Planta **210,** 715–722.

Paris, N., Rogers, S.W., Jiang, L., Kirsch, T., Beevers, L., Phillips, T.E., and Rogers, J.C. (1997). Molecular cloning and further characterization of a probable plant vacuolar sorting receptor. Plant Physiol. **115,** 29–39.

Paris, N., Stanley, C.M., Jones, R.L., and Rogers, J.C. (1996). Plant cells contain two functionally distinct vacuolar compartments. Cell **85,** 563–572.

Park, M., Kim, S.J., Vitale, A., and Hwang, I. (2004). Identification of the protein storage vacuole and protein targeting to the vacuole in leaf cells of three plant species. Plant Physiol. **134,** 625–639.

Rizo, J., and Südhof, T.C. (1998). C_2-domains, structure and function of a universal Ca^{2+}-binding domain. J. Biol. Chem. **273,** 15879–15882.

Robinson, D.G., Hinz, G., and Holstein, S.E.H. (1998). The molecular characterization of transport vesicles. Plant Mol. Biol. **38,** 49–76.

Sha, B., Phillips, S., Bankaitis, V., and Luo, M. (1998). Crystal structure of the *Saccharomyces cerevisiae* phosphatidylinositol-transfer protein. Nature **391,** 506–510.

Skehel, P.A., Martin, K.C., Kandel, E.R., and Bartsch, D. (1995). A VAMP-binding protein from *Aplysia* required for neurotransmitter release. Science **269,** 1580–1583.

Staehelin, L.A. (1997). The plant ER: A dynamic organelle composed of a large number of discrete functional domains. Plant J. **11,** 1151–1165.

Takahashi, R., and Shimosaka, E. (1997). cDNA sequence analysis and expression of two cold-regulated genes in soybean. Plant Sci. **123,** 93–104.

Vitale, A., and Hinz, G. (2005). Sorting of proteins to storage vacuoles: How many mechanisms? Trends Plant Sci. **10,** 316–323.